

# Influence of the Zeolite Type on the Mechanical–Thermal Properties and Volatile Organic Compound Emissions of Natural-Flour-Filled Polypropylene Hybrid Composites

Hee-Soo Kim, Hyun-Joong Kim

Laboratory of Adhesion and Bio-Composites, Program in Environmental Materials Science, Seoul National University, Seoul 151-921, South Korea

Received 28 December 2007; accepted 15 May 2008

DOI 10.1002/app.28853

Published online 10 September 2008 in Wiley InterScience (www.interscience.wiley.com).

**ABSTRACT:** The physicomaterial properties, thermal properties, odor, and volatile organic compound (VOC) emissions of natural-flour-filled polypropylene (PP) composites were investigated as a function of the zeolite type and content. The surface area and pore structure of the natural and synthetic zeolites were determined by surface area analysis and scanning electron microscopy, respectively. With increasing natural and synthetic zeolite content, the tensile and flexural strengths of the hybrid composites were not significantly changed, whereas the water absorption was slightly increased. The thermal stability and degradation temperature of the hybrid composites were slightly increased with increasing natural and synthetic zeolite content. At natural and synthetic zeolite

contents of 3%, the various odors and VOC emissions of the polypropylene/rice husk flour and polypropylene/wood flour hybrid composites were significantly reduced because of the absorption of the odor and VOC materials in the pore structures of the natural and synthetic zeolites. These results suggest that the addition of natural and synthetic zeolites to natural-flour-filled thermoplastic polymer composites is an effective method of reducing their odor and VOC emissions without any degradation of their mechanical and thermal properties. © 2008 Wiley Periodicals, Inc. *J Appl Polym Sci* 110: 3247–3255, 2008

**Key words:** composites; mechanical properties; poly(propylene) (PP); thermal properties; zeolites

## INTRODUCTION

In recent years, ecofriendly composite materials derived from natural-fiber-filled and flour-filled polyolefin and biodegradable polymer composites have been recognized as very attractive materials for reducing the environmental problems associated with nonbiodegradable plastic.<sup>1–3</sup> Nonbiodegradable plastic wastes can be reused by being recycled into useful products instead of being buried, but only a minor portion of plastics is recyclable, and most still ends up in municipal burial sites.<sup>4,5</sup> Hence, there is increased interest in the use of biodegradable natural fibers and flours as reinforcing fillers in thermoplastic polymers. Therefore, composites made with natural fibers and natural flours as reinforcing fillers offer various benefits, such as easy availability, low manufacturing energy, low CO<sub>2</sub> emission, low weight and cost, renewability, and biodegradability.<sup>6</sup> Rice husk flour (RHF) and wood flour (WF) are completely biodegradable biomass materials when used as natural flours in a wide variety of environments. In particular, RHF has the additional advantage of being an agrowaste material that is widely available

as a surplus byproduct of the rice production process.<sup>7</sup> Therefore, research has continued in an attempt to increase the use of RHF and WF as reinforcements for composites materials to increase their industrial applications. Polypropylene (PP) is a widely used matrix polymer in natural-filler-reinforced composites because of its excellent mechanical properties, thermal properties, light weight, chemical resistance, low cost, ease of processing, and good recycling properties.<sup>8</sup> In addition, the use of inorganic fillers (CaCO<sub>3</sub>, talc, mica, etc.) in thermoplastic polymers has been widely studied in an attempt to reduce their cost and improve their toughness, stiffness, and heat resistance.<sup>9,10</sup>

This study investigated the use of porous inorganic fillers in natural-flour-filled PP composites to reduce the odor and volatile organic compound (VOC) emissions and to improve the thermal properties. With increasing concerns about indoor air quality, reducing the VOC emissions of interior materials used as automotive parts and in buildings has become widely recognized as an important factor for interior materials.<sup>11,12</sup> In recent years, little attention has been focused on reducing the odor and VOC emissions of natural-filler-filled thermoplastic polymer composites or the use of porous inorganic fillers as reinforcing fillers in a natural-flour-filled PP composite system. In the melt-mixing process of

Correspondence to: H.-J. Kim (hjokim@snu.ac.kr).

TABLE I  
Chemical Compositions of the Natural and Synthetic Zeolites (wt %)

Element	SiO <sub>2</sub>	Al <sub>2</sub> O <sub>3</sub>	TiO <sub>2</sub>	Fe <sub>2</sub> O <sub>3</sub>	MgO	CaO	Na <sub>2</sub> O	K <sub>2</sub> O	MnO	P <sub>2</sub> O <sub>5</sub>	Loss on ignition	Total
Natural	59.9	16.2	0.4	3.9	1.9	4.4	2.9	1.6	0.1	0.1	9.4	100.8
Synthetic	54.5	2.2	0.1	1.4	28.9	3.5	—	0.01	0.02	0.1	8.6	99.3

natural-filler-filled thermoplastic polymer composites with a twin-screw extruder, odors and various VOCs are emitted by the natural filler because of the low degradation temperature of natural fillers.<sup>13</sup> In addition, VOCs are emitted from PP because of the random chain scission of the PP main chain and oxidation resulting from the high manufacturing temperature.<sup>14,15</sup> In this work, we used natural and synthetic zeolites as porous inorganic fillers to reduce the odor and VOC emissions and increase the thermal properties of natural-flour-filled PP composites. Natural and synthetic zeolites, which are crystalline inorganic materials possessing a high SiO<sub>2</sub>/Al<sub>2</sub>O<sub>3</sub> ratio and a three-dimensional network system of large pore channels, have attracted considerable technological interest.<sup>16</sup> These pores have variable openings, depending on the structure type, usually featuring internal cavities of variable shapes and diameters.<sup>17</sup> These pores are mainly composed of a microporous crystalline structure that is able to adsorb species that have diameters which fit through the surface entry channels.<sup>18</sup> In particular, synthetic zeolites (silver zeolite) have several advantages such as germicidal, bactericidal, antifungal, and antiseptic components in different compositions.<sup>8</sup> Therefore, we would expect the pore structures of natural and synthetic zeolites to absorb the VOCs emitted from the composites during the manufacturing process.

The aim of this study was to investigate the effect of the zeolite type on the physicomechanical properties, thermal properties, and VOC emissions of natural-flour-filled PP hybrid composites. This investigation was focused on reducing the various odors and VOC emissions of PP-RHF and PP-WF composites with natural and synthetic zeolites. The generated odor and VOC emissions of natural-zeolite-treated, synthetic-zeolite-treated, and nontreated composites were measured with a gas chromatograph coupled to a mass selective detector (GC-MSD). In addition, the physicomechanical properties and thermal properties of the zeolite-treated and nontreated composites were investigated.

## EXPERIMENTAL

### Materials

RHF and WF, purchased from Saron Filler Co. (Ansung, Kyungki, South Korea), were used as the reinforcing fillers. The particle sizes of RHF and WF

ranged from 860 to 270 and 110  $\mu\text{m}$ , respectively. PP was supplied by Hyosung Co. (Ulsan, Kyungnam, South Korea). It had a melt flow index of 1.7 g/10 min (190°C/2160 g) and a density of 0.91 g/cm<sup>3</sup>. The natural and synthetic zeolites were obtained from AutoWin Co. (Seoul, South Korea). The average particle sizes of the natural and synthetic zeolites were over 7.7 and 9.7  $\mu\text{m}$ , respectively. The chemical compositions of the natural and synthetic zeolites were determined with an X-ray fluorescence spectrometer (XRF-1700, Shimadzu, Nakagyo, Kyoto, Japan). Table I shows that the natural zeolite had high concentrations of SiO<sub>2</sub> and Al<sub>2</sub>O<sub>3</sub>, whereas the synthetic zeolite had high concentrations of SiO<sub>2</sub> and MgO. The Fourier transform infrared (FTIR) spectra of the natural and synthetic zeolites were obtained with a Thermo Nicolet (Madison, WI) Nexus 870 FTIR spectrophotometer.

### Compounding and sample preparation

The RHF, WF, and natural and synthetic zeolites were oven-dried at 105°C for 24 h to adjust the moisture content to 1–3% and then stored in sealed polyethylene bags before they were compounded with PP in a laboratory-sized, corotating, intermeshing twin-screw extruder (length/diameter ratio = 40) with three general processes: melt blending, extrusion, and pelletizing. The extruder barrel was divided into eight zones, with the temperature in each zone being individually adjustable. The temperature of the mixing zone in the barrel was maintained at 190°C with a screw speed of 250 rpm. The extruded strand was cooled in a water bath and pelletized with a pelletizer. The extruded pellets were oven-dried at 80°C for 24 h and stored in sealed polyethylene bags to avoid unexpected moisture infiltration. The mixtures were prepared with a 30 wt % filler loading to incorporate the natural and synthetic zeolites at loadings of 1, 3, and 5 wt %. The extruded pellets were injection-molded into tensile (ASTM D 638) and three-point-bending (ASTM D 790) test bars with an injection molding machine (Bau Technology, Uljungbu, Kyungki, South Korea) at 190°C with an injection pressure of 1200 psi and a device pressure of 1500 psi. After injection molding, the test bars were conditioned before testing at 50  $\pm$  5% relative humidity for at least 40 h according to ASTM D 618-99.

### Analysis of the porous properties of the natural and synthetic zeolites

The surface area and pore structure of the natural and synthetic zeolites were determined by the measurement of the physical adsorption of nitrogen at 77 K in an adsorption analyzer (model ASAP 2020, Micrometrics, Newton, MA). The natural and synthetic zeolites were outgassed at 350°C before the nitrogen adsorption-desorption experiments. The surface area was calculated according to the standard Brunauer-Emmett-Teller (BET) method. The total pore volume was estimated by measuring the volume of gas adsorbed at a relative pressure of  $P/P_0$  ratio of 0.998. The pore size distributions were determined with the Barrett-Joyner-Halenda method. Scanning electron microscopy (SEM) was used to measure the porous surfaces of the natural and synthetic zeolites with a Sirmom scanning electron microscope (FEI Co., Hillsboro, OR).

### Mechanical property tests of the composites

The tensile test for the composites was conducted according to ASTM D 638-99 with a Universal Testing Machine (Zwick Co., Ulm, Germany) at a crosshead speed of 5 mm/min and a temperature of  $20 \pm 2^\circ\text{C}$ . Composite specimens with a span-to-depth ratio of 16 : 1 underwent three-point-bending testing in accordance with ASTM D 790 at a crosshead speed of 5 mm/min. Five measurements were conducted and averaged for the final result.

### Water absorption test of the composites

Rectangular specimens (35 mm  $\times$  12 mm  $\times$  3 mm) were used in the water absorption tests. The samples were immersed in distilled water at 25°C for up to 50 days. At each testing time, the samples were removed from the water and patted dry, and the mass change was recorded with an electronic balance. The water absorption of the composites was calculated as the weight difference and reported as the percentage increase with respect to the initial weight.

### Thermal properties

Thermogravimetric analysis (TGA)

TGA measurements were carried out with a thermogravimetric analyzer (TGA Q500, TA Instruments, New Castle, DE) on 10-mg samples from 25 to 800°C (natural and synthetic zeolites) and from 25 to 700°C (composites) at a heating rate of 20°C/min. TGA was conducted with the compounds placed in a high-quality nitrogen (99.5% nitrogen, 0.5% oxygen) atmosphere with a flow rate of 20 mL/min to avoid unwanted oxidation.

### GC-MSD analysis

The GC-MSD analysis of the composites was performed on a CP-3800 gas chromatography/Saturn 2000 mass selective detector with a CP SIL 5CB capillary column (Varian Inc., Palo Alto, CA). Helium at a flow rate of about 1.2 mL/min was the carrier gas. The gas chromatography oven was initially held at 35°C for 5 min, then raised to 250°C at a rate of 8°C/min, and finally maintained at this temperature for 30 min. The bake-out time was increased to 30 min. The bake-out temperature was kept constant at 200°C. The mass spectrometry acquisition parameters, including scanning from  $m/z = 30$  amu to  $m/z = 650$  amu, were maintained in the electron impact mode automatically. High-quality nitrogen gas was injected into an odorless polyester bag containing the seven natural-zeolite-treated, synthetic-zeolite-treated, and nontreated PP-RHF and PP-WF composites. After they were maintained at 100°C for 24 h, the various odors and VOC emissions of the composites were analyzed with GC-MSD.

## RESULTS AND DISCUSSION

### Chemical structures and porous properties of the natural and synthetic zeolites

Figure 1 shows the FTIR spectra of the natural and synthetic zeolites. The absorption bands in the region of 3600–3300  $\text{cm}^{-1}$  were assigned to the hydroxyl (OH) groups bonding to silicon in the natural and synthetic zeolites. Furthermore, the synthetic zeolite showed a sharp peak at 3677  $\text{cm}^{-1}$  that was associated with Mg-OH groups.<sup>19</sup> The absorption band at 1016  $\text{cm}^{-1}$  was attributed to the internal tetrahedron symmetric stretch Si-O vibrations of the natural zeolites.<sup>16</sup> Also, this figure shows a new band at 667  $\text{cm}^{-1}$  for the synthetic zeolite. This band might be due to the Si-O(Mg)-O vibrations of the

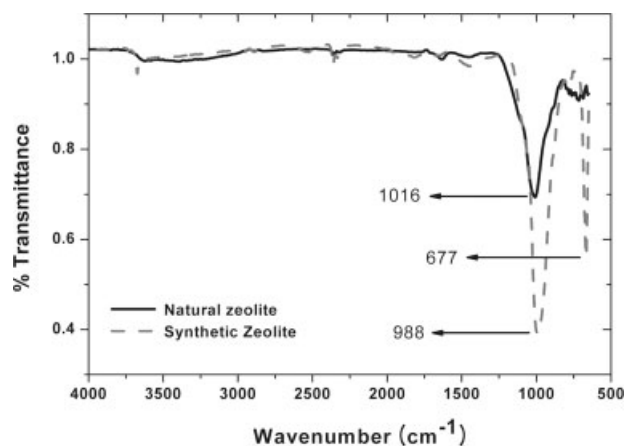


**Figure 1** FTIR spectra of the natural and synthetic zeolites.

**TABLE II**  
**BET Surface Areas and Average Pore Diameters**  
**of the Natural and Synthetic Zeolites**

Sample	BET surface area (m <sup>2</sup> /g)	Average pore diameter (nm)
Natural zeolite	32.7	7.8
Synthetic zeolite	2.1	21.9

synthetic zeolite. These results confirm the presence of these functional groups in the natural and synthetic zeolites. The application of the simple gas adsorption technique to a porous inorganic filler yields some basic structural information, such as the BET surface area, mean pore size, pore size distribution, and total pore volume.<sup>17</sup> Table II shows the BET surface areas and average pore diameters of the natural and synthetic zeolites. The BET surface area of the synthetic zeolite was smaller than that of the natural zeolite because the surface areas of the natural and synthetic zeolites depended on the inner spaces of their pores.<sup>20</sup> This result indicated that the larger surface area of the natural zeolite was due to its smaller pore size versus that of the synthetic zeolite. Figure 2(a,b) presents the curves of the pore vol-

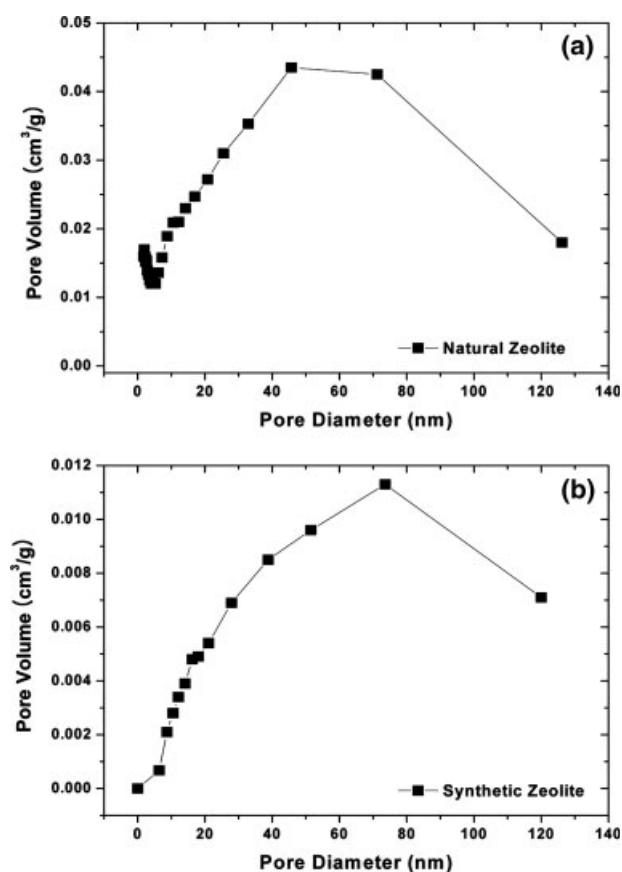


**Figure 2** Curves of the pore volume distribution as a function of the pore diameter for (a) the natural zeolite and (b) synthetic zeolite.

ume distribution as a function of the pore diameter for the natural and synthetic zeolites. The natural zeolite showed a smaller pore diameter throughout its porous structure than the synthetic zeolite. This result was confirmed by the SEM micrographs of the natural and synthetic zeolites in Figure 3, which show the existence of the porous structure. The pore sizes of the natural and synthetic zeolites were 20–50 and 74 nm, respectively, indicating a wider variation of pore sizes and a smaller pore size for the natural zeolite than for the synthetic zeolite. This result was also confirmed by the BET surface areas and average pore sizes of the natural and synthetic zeolites. The low surface area and pore volume of the synthetic zeolite and its relatively large mean pore diameter indicated the presence of mesopores and macropores in its structure. According to the International Union of Pure and Applied Chemistry classification,

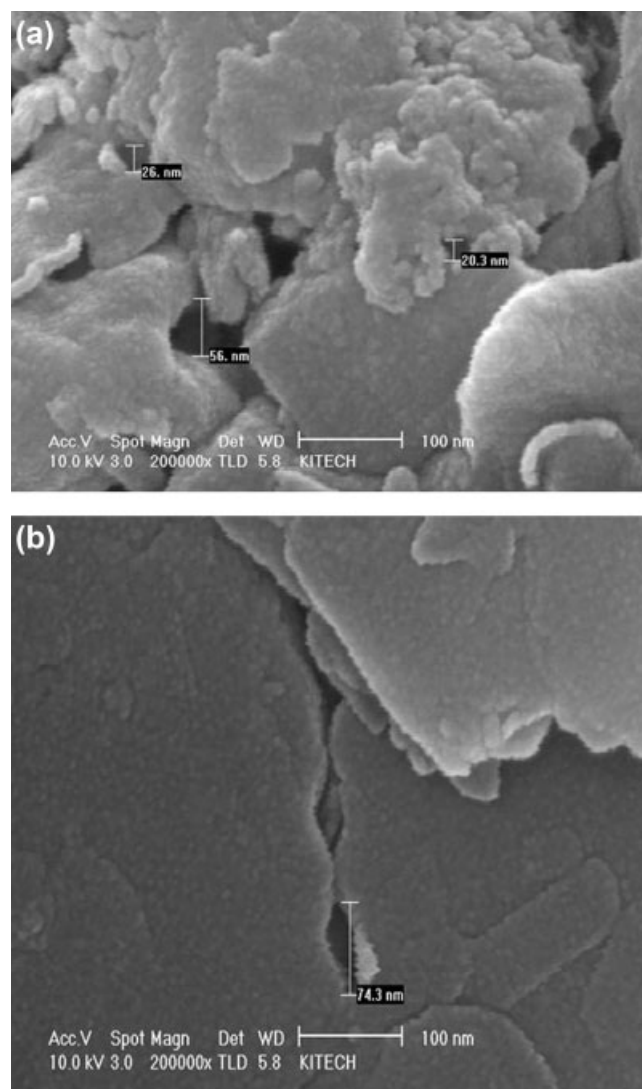


**Figure 3** SEM micrographs of (a) the natural zeolite and (b) the synthetic zeolite (100 nm).

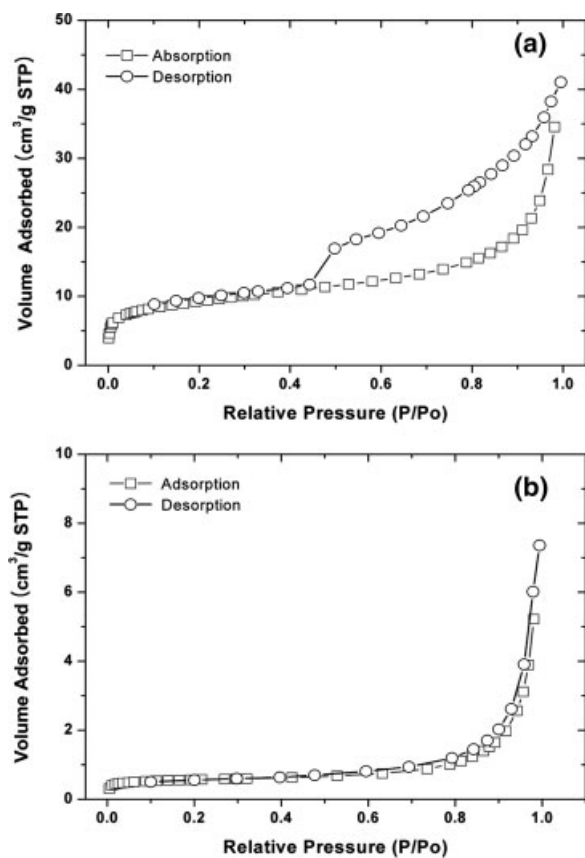


Figure 4 Adsorption-desorption isotherms of nitrogen on (a) the natural zeolite and (b) the synthetic zeolite at 77 K.

mesopores are pores with a diameter in the range of 20–50 nm, and macropores are pores whose radius is larger than 50 nm.<sup>20</sup> Thus, the average pore diameter and pore size distribution of inorganic porous materials are important factors for absorbing the emitted odors and VOCs of composites during the manufacturing process. The adsorption-desorption isotherms of nitrogen on the natural and synthetic

zeolites at 77 K are presented in Figure 4(a,b), respectively. The sharply increased adsorption of the natural and synthetic zeolites at a low relative pressure (0.0–0.2  $P/P_0$ ) was mainly due to adsorption in the micropores. The other region of increasing slope (above a  $P/P_0$  ratio of 0.8) was due to multilayer adsorption on the external surface.<sup>20</sup> Figure 4(a,b) also shows the hysteresis loops in the adsorption-desorption isotherms on the natural and synthetic zeolites, respectively. The hysteresis loop in the isotherm of the natural zeolite was wider than that in the isotherm of the synthetic zeolite, and this indicated that the former contained more micropores than the latter; this proved that the natural zeolite had a far larger pore volume than the synthetic zeolite.<sup>20–22</sup>

**Mechanical properties**

Figures 5 and 6 show the tensile and flexural strengths of the PP-RHF and PP-WF hybrid composites with different zeolite types and contents. As the content of natural and synthetic zeolites increased, the tensile and flexural strengths of the PP-RHF and PP-WF hybrid composites showed very little change. This indicated that the particle size of the synthetic and natural zeolites did not affect the mechanical properties because of the low concentration of natural and synthetic zeolites and that no interfacial interaction occurred between the hydrophilic inorganic porous filler and the hydrophobic PP matrix. In this study, the tensile and flexural strengths of the WF-filled PP composites were slightly higher than those of the RHF-filled PP composites, probably because of the difference in the chemical constituents and particle size of natural flour. In a previous study, Kim et al.<sup>6</sup> reported that the tensile strength of WF-filled poly(butylene succinate) (PBS) composites was higher than that of RHF-

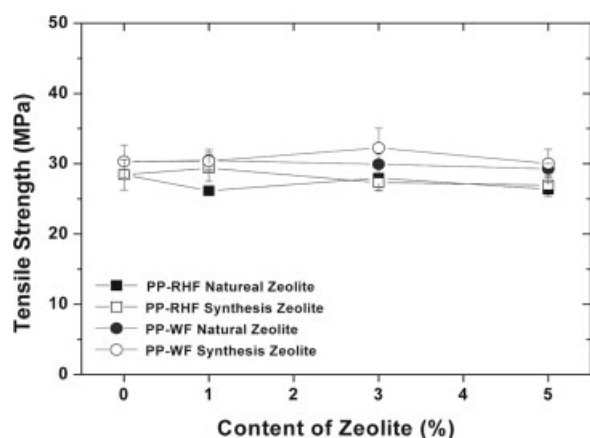


Figure 5 Tensile strength of PP-RHF and PP-WF hybrid composites with different zeolite types and contents.

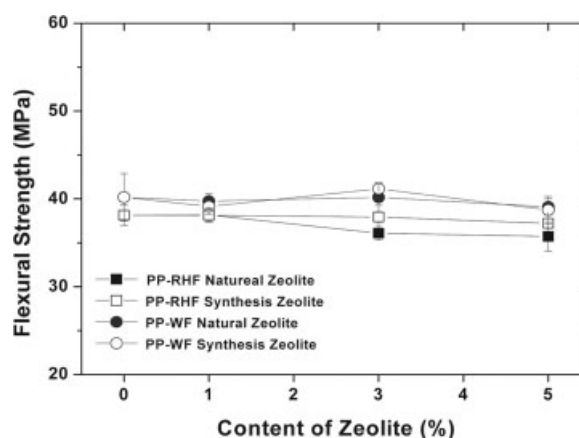
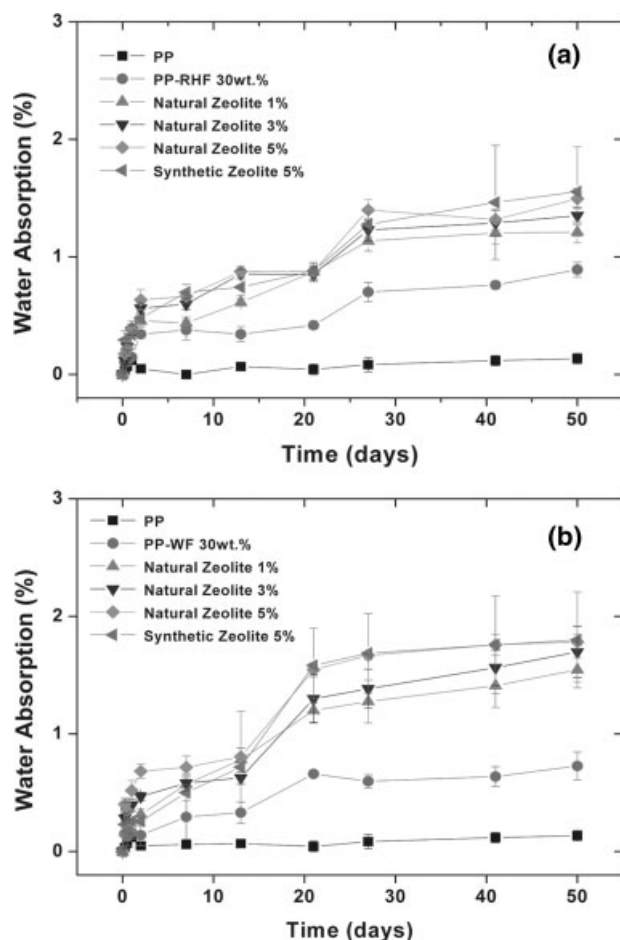


Figure 6 Flexural strength of PP-RHF and PP-WF hybrid composites with different zeolite types and contents.



**Figure 7** Water absorption curves of (a) PP-RHF and (b) PP-WF hybrid composites according to the zeolite type and content over a 50-day period.

filled PBS composites because WF showed higher holocellulose and lignin contents at the same particle size. Also, the tensile strength of the smaller RHF (80–100-mesh)-filled PBS composites was higher than that of the larger RHF (200-mesh)-filled PBS composites because the smaller RHF offered a larger specific surface area in the biocomposites than the larger RHF at the same weight fraction.<sup>6</sup>

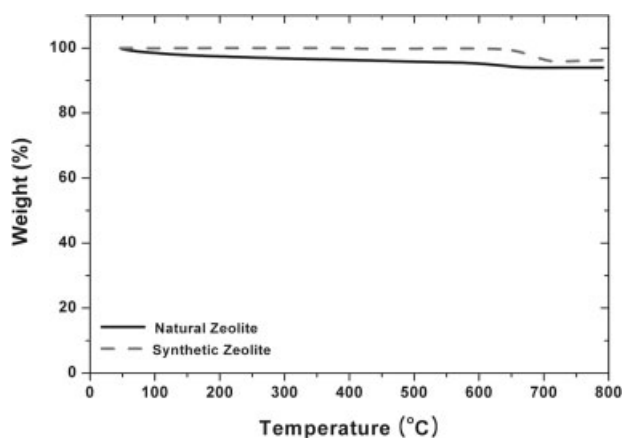
### Water absorption

Figure 7(a,b) shows the effects of the zeolite type and content on the water absorption curves of the PP-RHF and PP-WF hybrid composites over a period of 50 days. The absorption of water, which is mainly related to its rate of diffusion into the microgaps at the interface between the hydrophilic filler and thermoplastic polymer composite, causes undesirable dimensional changes in the final product and can degrade the mechanical properties by weakening the composites at the interface.<sup>8,23</sup> As shown in these figures, PP did not absorb any water because of its hydrophobic nature. The water absorption

increased rapidly with increasing water absorption time up to 27 days and thereafter remained almost constant. This result indicated that the hydroxyl (OH) groups of the natural flour and zeolite in the composites fully reacted with the water molecules. With increasing natural zeolite content, the water absorption slightly increased. The increased water absorption of the composites was due first to the hydrogen bonding between the hydroxyl (OH) groups introduced by the cellulose, hemicellulose, and lignin in the natural flour and the water molecules. Second, these hydroxyl groups, which absorbed water through the formation of hydrogen bonds, easily diffused into the natural-flour/matrix interface microgaps because of the low compatibility and adhesion of the two materials.<sup>23</sup> In addition, the water absorption of the hybrid composites slightly increased with increasing natural zeolite content because of the hydrophilic character and porous nature of the natural zeolite. The water absorption of the synthetic-zeolite-filled hybrid composites showed the same result. This result was confirmed by the presence of hydroxyl groups, such as Si–O(H)–Al and Si–O(H)–Mg, in the natural and synthetic zeolites, as indicated by the FTIR/attenuated total reflection analysis. At a synthetic and natural zeolite concentration of 5%, the water absorptions of the two types of hybrid composites were not significantly different, and this indicated that the water absorption of the hybrid composites increased with increasing porous inorganic filler content.<sup>8</sup>

### TGA

Figure 8 shows the dynamic TGA curves of the natural and synthetic zeolites. The weight losses of the natural and synthetic zeolites were about 6.0% and 3.6%, respectively, throughout the temperature range, indicating the gradual evaporation of



**Figure 8** TGA curves of the natural and synthetic zeolites.

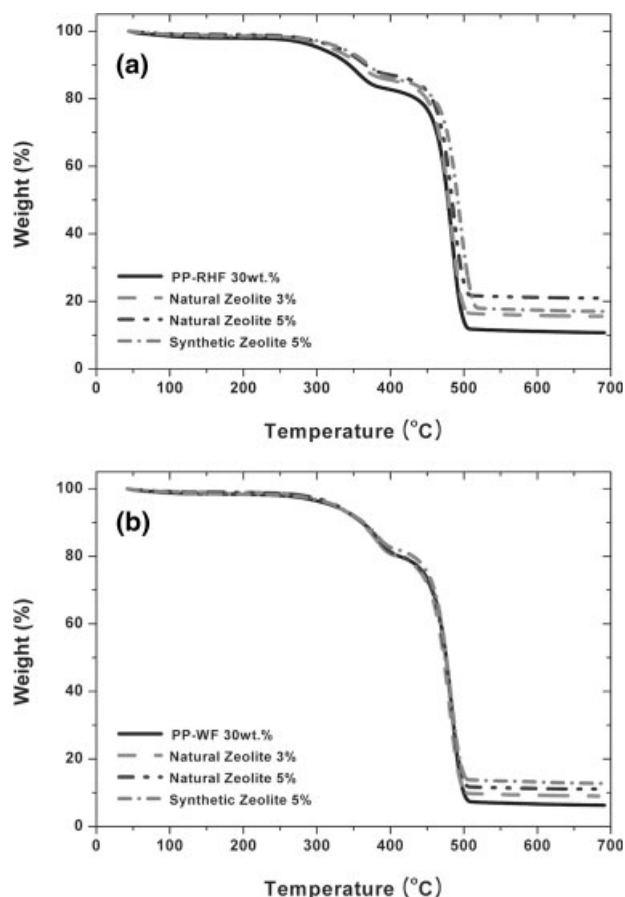


**Figure 9** TGA curves of (a) PP-RHF and (b) PP-WF hybrid composites with different zeolite types and contents.

moisture below 100°C and a further weight loss on the ignition of the organic materials in the temperature range of 100–800°C. The moisture contents of the natural and synthetic zeolites were 1.52% and 0.05%, and their inorganic material contents were 4.48% and 3.55%, respectively. These results indicate that the thermal stability of the synthetic zeolite was slightly higher than that of the natural zeolite because of the low organic material content of the former. Figure 9(a,b) shows the dynamic TGA curves of the PP-RHF and PP-WF hybrid composites, respectively, with different natural and synthetic zeolite types and contents. These figures show that the thermal degradation of the PP-RHF and PP-WF composites occurred in a two-step degradation process. The first thermal degradation step in the temperature range of 200–370°C was attributed to the hemicellulose, cellulose, and lignin constituents in RHF and WF, and the second one was attributed to the thermal degradation of PP, which was possibly due to the higher thermal stability and degradation temperature of PP versus those of natural flour.<sup>24</sup> With increasing natural and synthetic zeolite content, the thermal stability and degradation tem-

perature of the PP-RHF hybrid composites increased, and the mass residue (ash) content of the composites also increased. This result can also be seen in Table III. However, the thermal stability and degradation temperature of the PP-WF hybrid composites were not significantly changed with increasing natural zeolite content. At a natural and synthetic zeolite content of 5%, the weight-loss temperatures of the PP-WF hybrid composites were slightly increased. The enhanced thermal stability of the natural-zeolite-treated and synthetic-zeolite-treated composites can be attributed to the presence of quartz and the formation of metal oxides in the pozzolan, such as aluminum, ferrum, and magnesium oxides, on the PP and natural-flour surface.<sup>25</sup> In addition, the thermal stability of the PP-RHF and PP-WF hybrid composites was not significantly affected by the zeolite type because of the similar organic material contents of the natural and synthetic zeolites. These results suggest that the incorporation of inorganic porous materials as reinforcing fillers enhanced the thermal stability of the hybrid composites.

**GC-MSD analysis**

In this study, we measured the odor and VOC emissions of the PP-RHF and PP-WF hybrid composites at a natural and synthetic zeolite content of 3%. The test temperature was set at 100°C to investigate the effect of the high interior temperatures in the summer on automotive interiors. Table IV shows the furfural, limonene, and 5-methyl-2-furancarboxaldehyde emissions of the PP-RHF and PP-WF hybrid composites at a natural and synthetic zeolite content of 3%. Furfural, limonene, and 5-methyl-2-furancarboxaldehyde are the main materials that generate

**TABLE III**  
Mass Loss Temperature (°C) of Natural-Zeolite-Treated, Synthetic-Zeolite-Treated, and Nontreated PP-RHF and PP-WF Hybrid Composites

Sample	Mass loss temperature (°C)		
	5%	10%	20%
30 wt % PP-RHF	303.5	344.0	435.0
30 wt % PP-RHF (3% natural zeolite)	321.9	360.8	452.2
30 wt % PP-RHF (5% natural zeolite)	329.6	367.1	457.2
30 wt % PP-RHF (3% synthetic zeolite)	319.9	357.1	455.8
30 wt % PP-WF	322.3	361.4	412.1
30 wt % PP-WF (3% natural zeolite)	332.5	366.5	416.2
30 wt % PP-WF (5% natural zeolite)	331.7	366.9	419.6
30 wt % PP-WF (5% synthetic zeolite)	324.7	363.1	429.9

**TABLE IV**  
**Volatile Odor Compound Emissions of Natural-Zeolite-Treated,  
 Synthetic-Zeolite-Treated, and Nontreated PP-RHF and PP-WF Composites**

Detected item	Sample					
	30 wt % PP-RHF			30 wt % PP-WF		
	No treatment	Natural zeolite	Synthetic zeolite	No treatment	Natural zeolite	Synthetic zeolite
Furfural	1306	529	320	1397	512	493
Limonene	47	46	31	48	29	25
5-Methyl-2-furancarboxy aldehyde	30	7	6	75	17	21

the odor of the composites. Furfural can be produced from natural-filler materials rich in pentosan polymer, limonene is one of the most strongly emitted monoterpenes from wood and natural-filler materials, and 5-methyl-2-furancarboxyaldehyde is a volatile odor-active compound that is substantially responsible for its flavor.<sup>26–28</sup> Natural flour and PP can emit odors and VOCs because of the thermal degradation and oxidation of the natural-flour surfaces and the reaction of PP with the oxygen present during extrusion in the twin-screw extruder barrel at the high manufacturing temperature. The furfural and 5-methyl-2-furancarboxyaldehyde emissions of the natural-zeolite-treated and synthetic-zeolite-treated PP-RHF and PP-WF hybrid composites were significantly lower than those of the nontreated composites. Also, the limonene emission of the synthetic-zeolite-treated PP-RHF and natural-zeolite-treated and synthetic-zeolite-treated PP-WF hybrid composites was reduced, but that of the natural-zeolite-treated PP-RHF hybrid composites was not significantly changed. The reduced odor emission of these composites suggested that the volatile odor compounds and thermal degradation gases from the natural flour were absorbed into the pore structures of the natural and synthetic zeolites, and this

prevented them from migrating into the final products.<sup>15</sup>

Table V lists the emission levels, as detected by GC-MSD, of various VOCs from the natural-zeolite-treated, synthetic-zeolite-treated, and nontreated PP-RHF and PP-WF composites. At a natural and synthetic zeolite content of 3%, the VOC emissions of the PP-RHF and PP-WF hybrid composites were significantly decreased because of the porous natural and synthetic zeolites. The open porous structure of the porous inorganic natural and synthetic zeolites make them active as adsorbents.<sup>14,15</sup> This open porous structure could absorb the various VOC emissions and thermal degradation gases of the PP-RHF and PP-WF composites that were generated during the manufacturing process. The emission of 2-methyl furan, toluene, and 2-furan methanol from the natural-zeolite-treated hybrid composites was lower than that from the synthetic-zeolite-treated hybrid composites. However, the emission of benzyl alcohol from the synthetic-zeolite-treated hybrid composites was lower than that from the natural-zeolite-treated hybrid composites. These results demonstrate the variation in the pore size of the natural and synthetic zeolites, which is strictly connected to their structure.<sup>19</sup> Therefore, our study results confirm that

**TABLE V**  
**Various VOC Emissions from Natural-Zeolite-Treated, Synthetic-Zeolite-Treated,  
 and Nontreated PP-RHF and PP-WF Hybrid Composites**

Detected item	Sample					
	30 wt % PP-RHF			30 wt % PP-WF		
	No treatment	Natural zeolite	Synthetic zeolite	No treatment	Natural zeolite	Synthetic zeolite
Acetic acid	1132	855	754	690	307	342
2-Methyl furan	21	7	20	16	2	3
Toluene	132	113	130	126	128	132
2-Furan methanol	253	33	40	227	50	73
1,2-Furanyl ethanone	15	6	4	37	12	9
Benzyl alcohol	89	63	21	176	86	23
Azulene	67	63	62	76	39	40
Tetradecene	39	16	17	62	12	11

the addition of natural and synthetic zeolites is an effective method of reducing the odor and VOC emissions of natural-flour-filled thermoplastic polymer composites and therefore support their application as automotive interior and building interior materials.

### CONCLUSIONS

The BET surface area of the synthetic zeolite was smaller than that of the natural zeolite because of the latter's smaller pore size structure. The lower surface area and pore volume of the synthetic zeolite and its relatively large mean pore diameter confirmed the presence of mesopores and macropores in its structure. The hysteresis loop in the isotherm of the natural zeolite was wider than that in the isotherm of the synthetic zeolite, and this indicates that the former contained more micropores than the latter. With increasing natural and synthetic zeolite content, the tensile and flexural strengths of the PP-RHF and PP-WF composites were not significantly changed. This result indicates that the addition of natural and synthetic zeolites to the manufacturing process of the composites to reduce their odor and VOC emissions did not negatively affect their mechanical properties. With increasing natural and synthetic zeolite content, the water absorption and thermal stability of the hybrid composites was slightly increased. At a natural and synthetic zeolite content of 3%, the odor and VOC emissions of the hybrid composites were significantly decreased because the various oxidation and thermal degradation gases of the natural flour and matrix were absorbed into the pore structures of the natural and synthetic zeolites and thereby prevented from migrating into the final products. Therefore, we concluded that the addition of porous inorganic materials is an effective method of reducing the odor and VOC emissions of natural-flour-filled thermoplastic polymer composites in the manufacturing process.

### References

1. Ochi, S. *Compos A* 2006, 37, 1879.
2. Bhardwaj, R.; Mohanty, A. K.; Drzal, L. T.; Pourboghrat, F.; Misra, M. *Biomacromolecules* 2006, 7, 2044.
3. Ndazi, B.; Tesha, J. V.; Bissanda, E. T. N. *J Mater Sci* 2006, 41, 6984.
4. Kim, E. G.; Kim, B. S.; Kim, D. S. *J Appl Polym Sci* 2007, 103, 928.
5. Liao, H. T.; Wu, C. S. *Macromol Mater Eng* 2005, 290, 695.
6. Kim, H.-S.; Yang, H.-S.; Kim, H.-J. *J Appl Polym Sci* 2005, 97, 1513.
7. Vlaev, L. T.; Markovska, I. G.; Lyubchev, L. A. *Thermochim Acta* 2003, 406, 1.
8. Pehlivan, H.; Balkose, D.; Ulku, S.; Tihminlioglu, F. *J Appl Polym Sci* 2006, 99, 143.
9. Othman, N.; Ismail, H.; Mariatti, M. *Polym Degrad Stab* 2006, 91, 1761.
10. Toro, P.; Quijada, R.; Peralta, R.; Yazdani-Pedram, M. *J Appl Polym Sci* 2007, 103, 2343.
11. Yu, C. W. F.; Crump, D. R. *Indoor Built Environ* 2003, 12, 299.
12. Bledzki, A. K.; Faruk, O.; Sperber, V. E. *Macromol Mater Eng* 2006, 291, 449.
13. Calderia, I.; Caldeira, M. C.; Sousa, R. B.; Belchior, A. P. *J Food Eng* 2006, 76, 202.
14. Andersson, T.; Wessle, B.; Sandstro, J. *J Appl Polym Sci* 2002, 86, 1580.
15. Andersson, T.; Nielsen, T.; Wesslen, B. *J Appl Polym Sci* 2005, 97, 847.
16. Duvarci, O. C.; Akdeniz, Y.; Ozmihci, F.; Ulku, S.; Balkose, D.; Ciftcioglu, M. *Ceram Int* 2007, 35, 795.
17. Lee, J. F.; Lee, C. K.; Juang, L. C. *J Colloid Interface Sci* 1999, 217, 172.
18. Turn, N. G. *Bioresour Technol* 2008, 99, 2097.
19. Foster, M.; Furse, M.; Passno, D. *Surf Sci* 2002, 502, 102.
20. Majchrzak-Kuceba, I.; Nowak, W. *Thermochim Acta* 2005, 437, 67.
21. Lee, J. S.; Suh, J. K.; Hong, J. S.; Lee, C. H.; Lee, J. M. *J Ind Eng Chem* 2004, 4, 623.
22. Choi, D. H.; Park, J. W.; Kim, J. H.; Sugi, Y.; Seo, G. *Polym Degrad Stab* 2006, 91, 2860.
23. Espert, A.; Vilaplana, F.; Karlsson, S. *Compos Part A* 2004, 35, 1267.
24. Kim, H.-S.; Yang, H.-S.; Kim, H.-J.; Park, H.-J. *J Therm Anal Calorim* 2004, 76, 395.
25. Othman, N.; Ismail, H.; Mariatti, M. *Polym Degrad Stab* 2006, 91, 672.
26. Dias, A.; Pillinger, A.; Valente, A. *J Catal* 2005, 229, 414.
27. Linuma, Y.; Muller, C.; Boge, O.; Gnauk, T.; Herrmann, H. *Atmos Environ* 2007, 41, 5571.
28. Ranau, R.; Steinhart, H. *Eur Food Res Technol* 2005, 220, 226.